Acta Biochim Biophys Sin 2011, 43: 729–737 | © The Author 2011. Published by ABBS Editorial Office in association with Oxford University Press on behalf of the Institute of Biochemistry and Cell Biology, Shanghai Institutes for Biological Sciences, Chinese Academy of Sciences. DOI: 10.1093/abbs/gmr067.
Advance Access Publication 31 July 2011

Original Article

# Interactions of biocidal guanidine hydrochloride polymer analogs with model membranes: a comparative biophysical study

Zhongxin Zhou[1], Anna Zheng[2], and Jianjiang Zhong[1,3]*

[1]State Key Laboratory of Bioreactor Engineering, School of Bioengineering, East China University of Science and Technology, Shanghai 200237, China
[2]Key Laboratory for Ultrafine Materials, Ministry of Education, School of Materials Science and Engineering, East China University of Science and Technology, Shanghai 200237, China
[3]State Key Laboratory of Microbial Metabolism, School of Life Sciences & Biotechnology, Shanghai Jiao Tong University, Shanghai 200240, China
*Correspondence address. Tel: +86-21-34206968; Fax: +86-21-34204831; E-mail: jjzhong@sjtu.edu.cn

**Four synthesized biocidal guanidine hydrochloride polymers with different alkyl chain length, including polyhexamethylene guanidine hydrochloride and its three new analogs, were used to investigate their interactions with phospholipids vesicles mimicking bacterial membrane. Characterization was conducted by using fluorescence dye leakage, isothermal titration calorimetry, and differential scanning calorimetry. The results showed that the gradually lengthened alkyl chain of the polymer increased the biocidal activity, accompanied with the increased dye leakage rate and the increased binding constant and energy change value of polymer–membrane interaction. The polymer–membrane interaction induced the change of pretransition and main phase transition (decreased temperature and increased width) of phospholipids vesicles, suggesting the conformational change in the phospholipids headgroups and disordering in the hydrophobic regions of lipid membranes. The above information revealed that the membrane disruption actions of guanidine hydrochloride polymers are the results of the polymer's strong binding to the phospholipids membrane and the subsequent perturbations of the polar headgroups and hydrophobic core region of the phospholipids membrane. The alkyl chain structure significantly affects the binding constant and energy change value of the polymer–membrane interactions and the perturbation extent of the phospholipids membrane, which lead to the different biocidal activity of the polymer analogs. This work provides important information about the membrane disruption action mechanism of biocidal guanidine hydrochloride polymers.**

*Keywords* biocidal action mechanism; guanidine polymer; membrane interaction

Received: February 14, 2011 Accepted: May 27, 2011

## Introduction

The development of novel antimicrobial agents has been urgently required due to the continually emerging new antibiotic resistance mechanism [1] and the gradual reduction of new antimicrobial agents being brought to market [2]. Cationic amphiphilic antimicrobial polymers are currently receiving more attention as a new generation of antimicrobials in the field of antimicrobial drugs [3,4] and sterile-surface materials [5,6]. However, related publications mainly focused on the synthesis aspects of their novel molecular structures [7], which led to the lack of action mechanism studies.

As a kind of cationic antimicrobial polymer, polyhexamethylene guanidine hydrochloride (PHMG) possesses great potential in the development of highly effective antimicrobials [8–13] and covalently binds permanent sterile-surface materials [14,15] for hospital infection control. We have recently reported that the cytoplasmic membrane disruption of bacteria cells induced by PHMG–membrane interactions is the main antibacterial mechanism by micrographic observations of *Escherichia coli* cells exposed to PHMG [9,16]. However, a detailed characterization of interactions between the guanidine hydrochloride polymer molecule and the phospholipid membrane has not yet been performed.

Guanidine-containing derivatives constitute a very important class of antibacterial, antiviral, antiparasitic, and anticancer therapeutic agents [17–19]. The excellent antimicrobial property of PHMG and extensive bioactivities [17,20] of guanidine compounds inspire researchers to develop novel guanidine hydrochloride polymer analogs which would be expected to have higher antimicrobial potency. To achieve this goal, a comparative study on biocidal action mechanisms of different guanidine hydrochloride

polymer analogs is needed for gaining an extensive understanding about their membrane interactions.

The antimicrobial actions of a few cationic antimicrobial polymers are mainly attributed to the interactions between the polymer molecule and the phospholipid membrane [21]. This kind of membrane interactions has been characterized based on phospholipid model membrane system and biophysical techniques, e.g. encapsulated fluorescence dye leakage [22–24], isothermal titration calorimetry (ITC) [25,26] and differential scanning calorimetry (DSC) [27,28]. Both 1-palmitoyl-2-oleoyl-sn-glycero-3-phosphoethanolamine (POPE)/1-palmitoyl-2-oleoyl-sn-glycero-3-phosphoglycerol (POPG) (molar ratio 7:3) [25] and 1,2-dimyristoyl-sn-glycero-3-phospho-(1′-rac-glycerol) (DMPG) [27] phospholipid vesicles have been used as models of bacterial membrane. However, there has been no report on the interactions between the guanidine hydrochloride polymers and the model phospholipid vesicles [29].

In the present study, the interactions of PHMG and its three new analogs with model phospholipid vesicles were characterized by using dye leakage, ITC, and DSC. Furthermore, the biocidal action mechanisms and the underlying causes for activity differences of these guanidine hydrochloride polymer analogs were investigated and discussed.

## Materials and Methods

### Reagents

Phospholipids, POPE, POPG, and DMPG were purchased from Avanti Polar Lipids Inc. (Alabaster, USA). Tris(hydroxymethyl)aminoethane was purchased from Sigma-Aldrich Co. (St. Louis, USA). All salts were of analytical purity. Double-distilled water from deionized water was used in all experiments.

### Synthesis of oligoguanidine polymers

Four guanidine hydrochloride polymer analogs, i.e. PHMG (Polymer $C_6$) and its three new analogs, including polybutamethylene guanidine hydrochloride (Polymer $C_4$), polyoctanethylene guanidine hydrochloride (Polymer $C_8$) and poly(m-xylylene guanidine hydrochloride [Polymer $C_{8(benzene)}$], were synthesized as shown in the Supplementary data.

### Antibacterial testing

The minimal inhibition concentration (MIC) of polymers was determined using the standard method of Muller Hinton Broth microdilution as described with minor modification [30]. Briefly, all polymers were dissolved in 10 mM phosphate buffer solution (PBS, pH 7.4) with final pH 7.4, respectively. Above solutions were further diluted with 10 mM PBS (pH 7.4) to obtain polymer solutions with a two-fold dilution series (0.5–2048 μg/ml). Bacteria were cultured on plate (5% sheep blood agar plate) overnight at 37°C, and the cultures were further suspended, centrifuged, and resuspended with 10 mM PBS (pH 7.4) for three cycles. The cell suspensions with an optical density of 0.35 at 600 nm, which corresponded to $2.5 \times 10^8$ colony forming unit (CFU) per milliliter based on the plate counts of *E. coli*, were then diluted to $\sim 5 \times 10^5$ CFU/ml in two-fold cation-adjusted Muller Hinton Broth (Oxoid Ltd, Basingstoke, England). MIC endpoints were read as the lowest antimicrobial concentration that completely inhibited macroscopically visible growth of the inoculum as suggested [8]. Chlorhexidine digluconate [CHG; 20%; Sigma-Aldrich (St. Louis, USA)], another member of the family of cationic antimicrobials and the most widely used biocide in antiseptic products, was taken as the reference substance.

Four reference strains for disinfectant, *E. coli* strain 8099 as a typical strain of intestinal bacteria, *Staphylococcus aureus* ATCC 6538 as a typical strain of pyogenic coccus, *Pseudomonas aeruginosa* ATCC 15442 as a typical strain in hospital, *Candida albicans* ATCC 10231 as a typical strain of pathogenic fungus, in Technical Standard for Disinfection (2002 edition, Ministry of Health, China), were provided by Shanghai Municipal Center for Disease Control & Prevention (Shanghai, China). The clinical strains of *P. aeruginosa* and *S. aureus* were provided by Huashan Hospital, Shanghai Medical College, Fudan University (Shanghai, China).

### Preparation of biomimetic vesicles

Homogeneous calcein-loaded large unilamellar vesicles (LUVs) were prepared by the extrusion method. The following buffers were used: buffer A (40 mM calcein, 10 mM Tris, pH 7.4) and buffer B (10 mM Tris, 150 mM NaCl, pH 7.4). About 10 mg POPE/POPG phospholipids mixtures (molar ratio 7:3) were dissolved in 10 ml chloroform/methanol mixture (volume ratio 2:1) in a 25 ml eggplant-type flask. The organic solvents were removed in 25°C water bath by rotary evaporator to form a uniform lipid film. Trace amounts of organic solvents were removed by placing the sample under vacuum overnight. The dried film was hydrated with 1 ml buffer A at 25°C (at least 10°C above the $T_m$ of the phospholipids) by vortex for about 30 min until the entire lipid film was removed from the walls of the flask and a homogenous multilamellar lipid vesicles (MLVs) suspension was formed. The MLVs suspension was subjected through five freeze/thaw cycles using liquid nitrogen and warm water. Further, the suspension was extruded 15 times through a Mini-Extruder equipped with a polycarbonate membrane filter with 1 μm pore diameter, then 15 times with a 400 nm filter, at room temperature, to form the LUVs. Finally, unencapsulated calcein was removed by gel filtration on a 1.6 × 40-cm

Sephadex G-50 superfine (~10 g) column at a flow rate of 0.5 ml/min, the fractions collected in the void volume were stored at 4°C and diluted as needed for up to 7 days. The concentration of phospholipid was determined by phosphate analysis [31], and the LUVs were diluted to appropriate concentration before measurement. For the *E. coli* total lipid extract-based LUVs, the preparation process was the same except different lipid being used.

LUVs for ITC were made as calcein-loaded LUVs. About 46 mg POPE/POPG dry lipids mixtures (molar ratio 7:3) was used, and the formed lipid film was hydrated with 2.2 ml buffer B.

Regarding the MLVs for DSC, they were prepared as the procedure mentioned above, while 15.8 mg DMPG phospholipids and 4.7 ml buffer B were used.

### Polymer-induced leakage assays of fluorescence dye

Fluorescence measurements were performed in an SLM Aminco Bowman Series II spectrofluorimeter (SLM Instruments, New York, USA), using an excitation wavelength of 490 nm and an emission wavelength of 515 nm with 5-nm bandwidth slits. LUVs were added to a quartz cuvette (2 ml total volume containing polymer, buffer B, and calcein-loaded LUVs) with a final concentration of 20 μM, leakage was initiated by addition of polymer with a final concentration of 10 μg/ml, and fluorescence was recorded at 30°C. For determination of 100% dye release, 20% Triton X-100 (50 μl) was added to dissolve the vesicles without addition of polymer. The percentage of dye leakage caused by polymers was calculated as follows: dye leakage $(\%) = 100 \times (F - F_0)/(F_t - F_0)$, where $F$ is the fluorescence intensity achieved by the addition of polymer, $F_0$ is the fluorescence intensities without any addition of polymers or Trition, and $F_t$ is the fluorescence intensities induced by the addition of 20% Triton X-100.

### Isothermal titration calorimetry

Titrations were performed in a VP-ITC instrument (MicroCal Inc., Northampton, USA) as suggested by Liang *et al.* [32] with minor modification. Prior to the measurement all solutions were degassed under vacuum for 15 min. Polymer solution at a concentration of 75 μg/ml dissolved in TBS (final pH 7.4) was placed in the 1.414 ml calorimeter cell. LUVs suspension (15 mM) was placed in the 295.66 μl syringe and injected over 20 s in aliquots of 10 μl (the first injection was 3 μl) with 300 s intervals between the individual injections. The syringe was assembled into the calorimeter cell for equilibrium while stirring at 300 rpm. The baseline heat signal (set at 15 μcal/s) and calorimeter cell temperature (set at 30°C) usually stabilized within 15–30 min. To account for the heat of dilution, control experiments were completed by titrating lipid vesicles into the TBS solution in the absence of polymers. Data acquisition and analysis were performed using Microcal Origin software (MicroCal). The 'One Set of Sites' binding model, provided with the software, was used. Enthalpy changes ($\Delta H$) were calculated from the sum of heats of reaction. Changes in free energies ($\Delta G$) and entropies ($\Delta S$) were calculated using the equation: $\Delta G = \Delta H - T\Delta S$.

### Differential scanning calorimetry

Measurements were made using a Differential Scanning Calorimetry (Micro DSCIII SETARAM Instrumentation, Caluire, France). The polymer was dissolved in TBS (adjusted final pH 7.4). The volume of MLVs samples loaded into the cell was 0.70 ml, which contained 1.87 mg lipid and 0.14 mg polymer. The lipid:polymer molar ratio was around 10:1. To better mimic the biological event, the biocidal polymer was added to the lipid after vesicle/liposome formation, and then the sample was balanced at 25°C for 2 h (to reduce the scan running) before loading to instrument. A scan rate of 0.5°C/min from −2 to 35°C was used with a 30 min delay between sequential scans in a series for thermal equilibration. Sample runs were performed three times to ensure reproducibility. The enthalpy values were obtained by the integration of area under the phase transition bands using instrument's software. Control samples containing the polymer alone at corresponding concentrations exhibited no thermal events over the temperature range from −2 to 35°C.

## Results

### Comparison of biocidal activities of Polymer $C_4$, $C_6$, $C_8$, and $C_{8(benzene)}$

As shown in **Table 1**, Polymer $C_4$, $C_6$, and $C_8$ displayed gradually increased biocidal activity with the increased alkyl chain length of the repeat unit of the polymer, and Polymer $C_8$ had higher activity than Polymer $C_{8(benzene)}$. The novel Polymer $C_8$ also exhibited higher biocidal activity than Polymer $C_6$ (PHMG) against Gram-negative and Gram-positive clinical strains and reference bacteria for disinfectant. The MIC values of the novel Polymer $C_8$ were between one half and one quarter that of PHMG or CHG.

### Dye leakage of model POPE/POPG (7:3) lipid vesicles

The leakage of fluorescent dye calcein encapsulated in the model lipid POPE/POPG (7:3) vesicles has been previously applied to monitor the membrane interactions of cationic antimicrobial polymer [22]. POPE/POPG vesicles have net negative surface charge because POPG lipids have anionic head groups. **Figure 1** shows that when four guanidine hydrochloride polymers were, respectively, added to the anionic POPE/POPG vesicles, calcein dye

**Table 1 Biocidal activities of synthesized Polymer $C_4$, $C_6$, $C_8$, and $C_8$(benzene)**

| Organism group and species | Strain isolate no. | Antibiotic resistance | MIC (μg/ml) | | | | |
|---|---|---|---|---|---|---|---|
| | | | $C_4$ | $C_6$ | $C_8$ | $C_{8(benzene)}$ | CHG |
| Reference strains for disinfectant | | | | | | | |
| Gram-negative species | | | | | | | |
| *Pseudomonas aeruginosa* ATCC 15442 | | | 171.0 | 8.0 | 4.0 | 32.0 | 8.0 |
| *Escherichia coli* 8099 | | | 64.0 | 8.0 | 2.7 | 16.0 | 8.0 |
| Gram-positive species | | | | | | | |
| *Candida albicans* ATCC 10231 | | | 32.0 | 2.0 | 1.0 | 4.0 | 8.0 |
| *Staphylococcus aureus* ATCC 6538 | | | 8.0 | 2.0 | 1.0 | 4.0 | 8.0 |
| Clinical strains | | | | | | | |
| Gram-negative species | | | | | | | |
| *P. aeruginosa* | 08–1636 | MDR[a] | 128.0 | 16.0 | 8.0 | 64.0 | 16.0 |
| *P. aeruginosa* | 09–107 | MDR | 128.0 | 16.0 | 8.0 | 64.0 | 16.0 |
| *P. aeruginosa* | 09–362 | MDR | 128.0 | 12.0 | 8.0 | 64.0 | 16.0 |
| Gram-positive species | | | | | | | |
| *Staphylococcus aureus* | 09–425 | MR[b] | 64.0 | 4.0 | 2.0 | 16.0 | 8.0 |
| *S. aureus* | 09–485 | MR | 64.0 | 8.0 | 4.0 | 16.0 | 16.0 |
| *S. aureus* | 09–421 | MR | 48.0 | 8.0 | 8.0 | 24.0 | 16.0 |

Chlorhexidine digluconate (CHG, 20%) was used as the reference substance. The minimal inhibition concentration (MIC) was the mean value from three independent experiments.

[a]Multidrug resistant.

[b]Meticillin resistant.

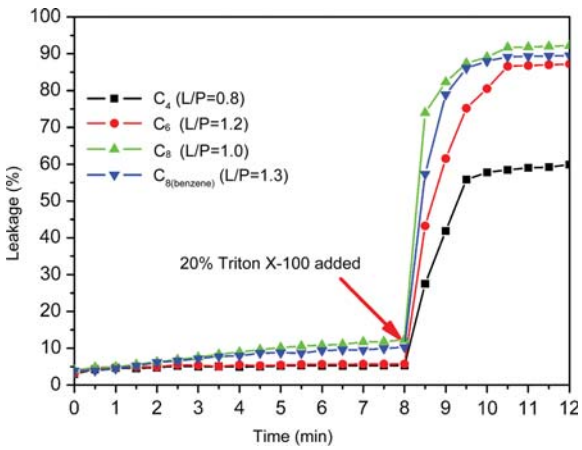


**Figure 1 Calcein fluorescence dye leakage of POPE/POPG (7:3) lipid vesicles after exposure to Polymer $C_4$, $C_6$, $C_8$, and $C_{8(benzene)}$** L/P is the molar ratio of lipid/polymer.

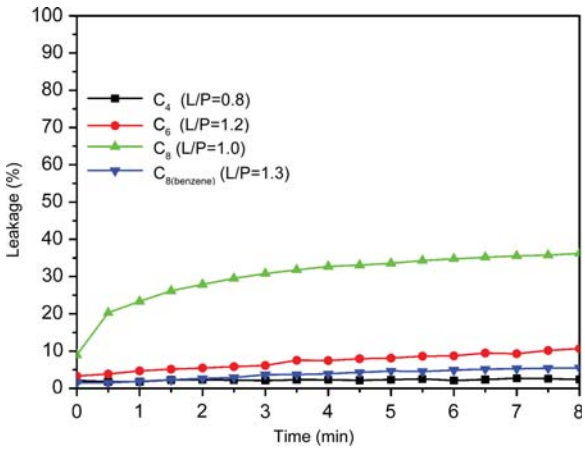


**Figure 2 Calcein fluorescence dye leakage of lipid vesicles composed of *E. coli* total lipid extract after exposure to Polymer $C_4$, $C_6$, $C_8$, and $C_{8(benzene)}$** L/P is the molar ratio of lipid/polymer.

leakage was induced ~5–10% leakage rate, and each leakage trace had an extremely slow increase trend throughout the 480-s time range. In spite of low dye leakage rate, the ability of Polymer $C_4$, $C_6$, and $C_8$ to induce dye leakage was positively correlated with the carbon chain length of the repeat unit of the biocidal polymer. Polymer $C_{8(benzene)}$ led to a relatively lower leakage rate than Polymer $C_8$.

## Dye leakage of model lipid vesicles of *E. coli* total lipid extract

To validate the dye leakage rate result of the above anionic POPE/POPG vesicles, vesicles composed of *E. coli* total lipid extract with more similarity to the bacterial membrane were prepared as reported [25]. As shown in **Fig. 2**, the calcein leakage traces of *E. coli* total lipid extract vesicles were almost the same as the corresponding traces of POPE/

POPG vesicles when exposed to Polymer $C_4$ and $C_6$. There were only delicate differences for the leakage rate induced by Polymer $C_8$ and Polymer $C_{8(benzene)}$, which could be accepted considering the actual differences between the natural *E. coli* total lipid extract vesicles and the model POPE/POPG vesicles. So the data of dye leakage rate of anionic POPE/POPG vesicles were reliable.

## ITC of membrane interactions

To investigate how the alkyl chain structure change of the polymer analog affects the thermodynamic process of polymer–lipid membrane interactions and the resulted different dye leakage rate and biocidal activity, ITC between the polymer analog and the phospholipid vesicles was performed. For the convenience of obtaining enough thermal signals and observing the thermodynamic difference of membrane interactions of four polymer analogs, the same high-polymer-concentration was used.

**Figure 3** showed the heat flow traces produced by titrating POPE/POPE LUVs into Polymer $C_4$ [**Fig. 3(A)**], $C_6$ [**Fig. 3(B)**], $C_8$ [**Fig. 3(C)**], and $C_{8(benzene)}$ [**Fig. 3(D)**] solutions and the total heat per injection at different lipid/polymer molar ratios. For Polymer $C_4$, $C_6$, and $C_8$, every single injection produced an endothermic reaction, the heat value of which gradually decreased with consecutive injections. Both Polymer $C_6$ and $C_8$ resulted in much larger endothermic heat value than Polymer $C_4$ for their initial corresponding 16 injections (data not shown, total 25 injections for each polymer). It was noted that Polymer $C_8$ induced more endothermic heat for the initial eight injections, while less endothermic heat for the subsequent 17 injections than Polymer $C_6$ (data not shown). So the heat value of the endothermic reaction induced by titrating POPE/POPG vesicles into the Polymer $C_8$ decreased more rapidly compared with the vesicles titrated into Polymer $C_6$ and $C_4$, which made the reaction of titration into Polymer $C_8$ reach saturation before the total 25 injections were completed, while no saturation point was observed for other polymers. Similar ITC traces have been shown for cationic antimicrobial peptides that have charged and hydrophobic moieties as cationic antimicrobial polymers, and are interpreted as a result of the binding process occurring along with other processes [25]. Our results suggested that Polymer $C_4$, $C_6$, and $C_8$ had different binding affinity for POPE/POPE vesicles, according to which they were arranged in the increasing order of Polymer $C_4$, $C_6$, and $C_8$. It was consistent with the circumstance that Polymer $C_8$ had a higher binding constant (3620/mol) than Polymer $C_6$ (1480/mol). The extremely low-binding affinity (too little energy change for different molar ratio) for Polymer $C_4$ [**Fig. 3(A)**] made it difficult to fit and derive the binding constant for the equipment. Therefore, only qualitative conclusions could be made in these cases. The titration reaction of POPE/POPG vesicles into Polymer $C_{8(benzene)}$ resulted in an exothermic effect with an initially increasing trend, which was followed by a gradually decreased exothermic heat after five injections.

## DSC of membrane interactions

DSC was performed to monitor the effects of four guanidine hydrochloride polymers on the thermotropic behavior

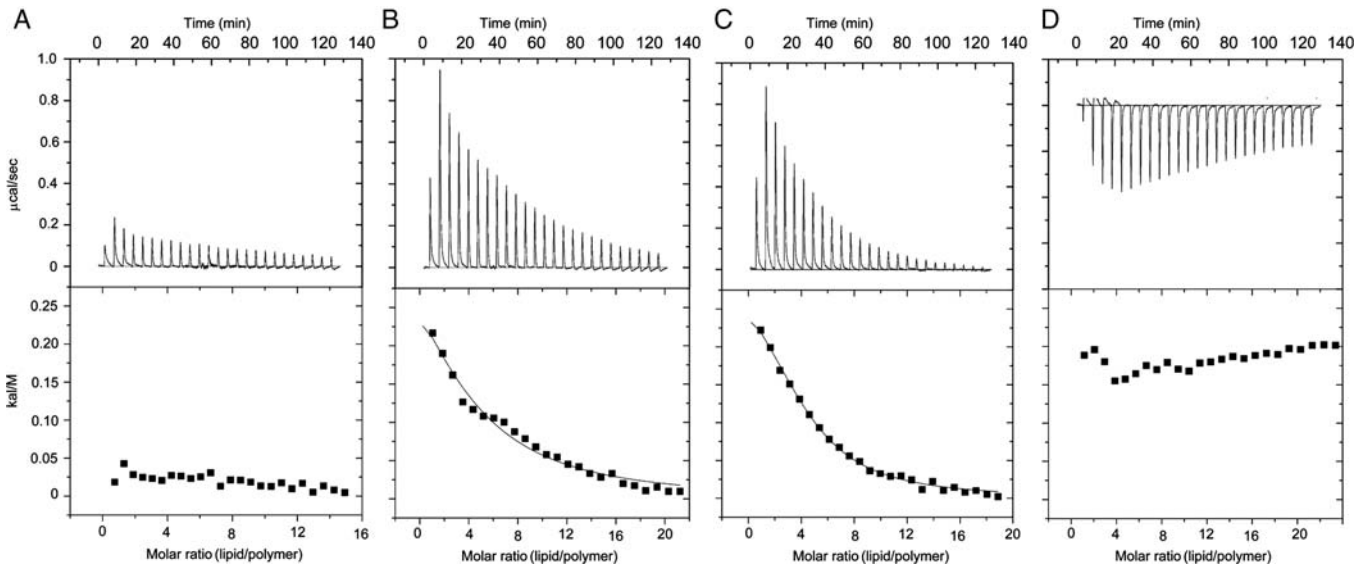


**Figure 3 Titration calorimetry of POPE/POPG (7:3) vesicles into Polymer $C_4$, $C_6$, $C_8$, and $C_{8(benzene)}$ solutions at 30°C** (A) Polymer $C_4$; (B) Polymer $C_6$; (C) Polymer $C_8$; and (D) Polymer $C_{8(benzene)}$; 75 μg/ml polymer and 15 mM lipid. The lower curve in each case represents the heat of reaction (measured by peak integration) as a function of the lipid/polymer molar ratio. The solid line is the best fit to the experimental data using the one site binding model.

of phospholipid vesicles, which could help to understand the sites of interactions between these polymers and the phospholipid membrane. DMPG MLVs were used for the DSC measurements because MLVs of POPE/POPG (molar ratio 7:3) in former measurement system had a phase transition temperature ~0–5°C (data not shown), which is near the solution temperature of ice, and the solution heat of ice can affect the results.

DSC thermograms representing the effects of four guanidine polymers on the thermal behavior of the DMPG vesicles were shown in **Fig. 4**. In the absence of guanidine polymers, DMPG MLVs exhibited two endothermic transitions, a weak energetic pretransition near 17°C (conversion of the ordered lamellar gel phase L$\beta'$ to the ordered rippled gel phase P$\beta'$) and a strong energetic and highly cooperative main phase transition near 23°C (conversion of the rippled gel phase to the fluid lamellar liquid-crystalline phase Lα), in agreement with previously published data [27]. As we know, the pretransition is due to interactions between the phospholipid headgroups, and the main phase transition (chain melting) is mainly due to *trans-gauche* interconversion of the acyl chains, which decreases the acyl chain packing of the lipid molecules and increases the fluidity of the membrane [33,34].

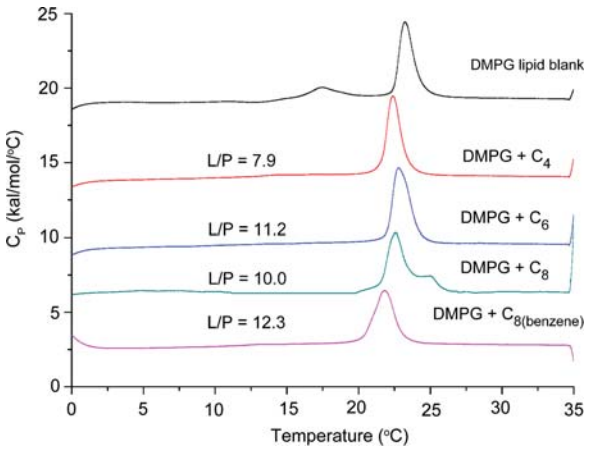


**Figure 4 Differential scanning calorimetry heating scans illustrating the effects of Polymer $C_4$, $C_6$, $C_8$, and $C_{8(benzene)}$ on the thermotropic phase behaviour of DMPG MLVs** L/P is the molar ratio of lipid/polymer. Each sample was 0.7 ml with 1.87 mg lipid and 0.14 mg polymer, and the control one was 0.70 ml with 1.87 mg lipid.

The addition of Polymer $C_4$, $C_6$, $C_8$, and $C_{8(benzene)}$ into the lipid vesicles strongly reduced the temperature, the enthalpy, and the cooperativity of the pretransition to different extent (**Fig. 4** and **Table 2**), indicating the existence of significant interactions between the polymer and the phospholipid headgroups. It was because that incorporation of the polymer molecule increased the distance between the phospholipid headgroups. As their interactions were weakened, a conformational change of the phospholipids headgroups was caused, and the pretransition change was thus produced [33].

For the main phase transition, the melting of the acyl chains of the phospholipid layers of Polymer $C_6$, $C_8$, and $C_{8(benzene)}$ was less cooperative (disordering) as demonstrated by the decreasing temperature and the increased half-width of the main transition peak compared with the control lipids (**Table 2**), which indicated that Polymer $C_6$, $C_8$, and $C_{8(benzene)}$ had strong interactions with the acyl chains hydrophobic domain of the phospholipids layers. It was suggested that both shifting toward lower temperature and broadening of the main transition peak indicated fluidification of the membrane and lower packing of the lipid molecules as a result of penetration of polymer molecules into the hydrophobic domain of the phospholipid membrane [33]. Despite the change in temperature and cooperativity of the main transition for Polymer $C_6$, $C_8$, and $C_{8(benzene)}$, the enthalpy remained close to that of pure DMPG, indicating that they decreased the apparent order of the hydrocarbon chains of the liquid crystalline lipid bilayers [33].

**Table 2 Thermotropic phase behavior of DMPG lipid vesicles upon addition of Polymer $C_4$, $C_6$, $C_8$, $C_{8(benzene)}$**

| | Pretransition | | Main transition | | |
|---|---|---|---|---|---|
| | $T_m^a$ (°C) | $\triangle H^b$ (kcal/mol) | $T_m$ (°C) | $\triangle H$ (kcal/mol) | Half-width (°C) |
| DMPG blank | 17.5 ± 0.03 | 1.8 ± 0.01 | 23.3 ± 0.05 | 6.4 ± 0.04 | 1.2 ± 0.07 |
| $C_4$ (L/P$^c$ = 7.9) | 14.1 ± 0.07 | 0.1 ± 0.00 | 22.4 ± 0.00 | 6.9 ± 0.05 | 1.1 ± 0.00 |
| $C_6$ (L/P = 11.2) | – | – | 22.7 ± 0.07 | 6.8 ± 0.04 | 1.3 ± 0.01 |
| $C_8$ (L/P = 10.0) | – | – | 22.6 ± 0.00 | 6.4 ± 0.04 | – |
| $C_{8(benzene)}$ (L/P = 12.3) | 12.9 ± 0.07 | 0.1 ± 0.00 | 21.8 ± 0.01 | 6.1 ± 0.09 | 1.6 ± 0.00 |

[a]Phase transition temperature ($T_m$).

[b]Total entalpy change ($\triangle H$).

[c]L/P is the molar ratio of lipid/polymer. Phase transition temperature and entalpy change were estimated by using the instrument's soft. Values were expressed as means ± SD.

## Discussion

In this study, four guanidine hydrochloride polymer analogs exhibited gradually increased biocidal activity with increasing alkyl chain length. Correspondingly, these polymer analogs disrupted the phospholipid vesicles mimicking bacteria membrane and induced encapsulated dye leakage to different extent at concentrations comparable to their MIC. The magnitude of biocidal activity of each analog and its ability to disrupt the model phospholipid membrane (dye leakage) were positively correlated with the binding affinity, which could be evaluated by binding constant and energy change value of the strong interactions between the polymer analog and the phospholipid membrane. The increasing alkyl chain length led to the increase of the binding affinity. Furthermore conformational change in the phospholipid headgroups and disordering in the hydrophobic regions of phospholipid membranes played important roles in the strong membrane interactions and biocidal actions of guanidine hydrochloride polymers.

ITC demonstrated the existing strong membrane interactions because the $\Delta H$ values were positive (endothermic effects) for binding of Polymer $C_4$, $C_6$, and $C_8$ to POPE/POPG vesicles. But actually the electronic interactions between the cationic polymer and the anionic headgroups of phospholipid molecules of POPE/POPG membrane were exothermic, and the heat effect detected by the ITC was overall heat changes [35]. It could be explained that, for Polymer $C_4$, $C_6$, and $C_8$ with enough conformational flexibility given by the linear alkyl chain, the energy released by the electronic interactions was not enough for these polymers' actions to disrupt the permeability barrier of the phospholipids membrane [16]. The following strong membrane interactions accompanied with additional energy absorbed from the system were necessary, which lead to the overall endothermic effect. But the rigid benzene ring of Polymer $C_{8(benzene)}$ limited the polymer's molecule motion and partition into the lipid membrane, and the heat released by electronic interactions was enough. So the titration of vesicles into Polymer $C_{8(benzene)}$ produced an entire exothermic effect (the $\Delta H$ value was negative). The endothermic effects indicated that the bindings were entropy-driven and entropically favorable [$\Delta S$, 16.3 and 17.4 kcal/(mol K) for Polymer $C_6$ and $C_8$, respectively]. Cationic polynorbornene (MIC 25 μg/ml) binding to POPE/POPG also produced strong endothermic effects [36].

Different from the above endothermic effects, most of cationic antimicrobial peptide binding to anionic lipids produced exothermic effects [25,37–39]. These peptides had MIC values from a few to hundreds of μg/ml against the Gram-negative bacteria, which were similar to the activity range of Polymer $C_4$, $C_6$, and $C_8$. So it was the structure of the compound, rather than the antimicrobial activity, determined the endothermic or exothermic effects.

The above-mentioned strong membrane interactions besides the electronic interactions between the polymer and the anionic headgroups of phospholipids may be the interactions existing between the polymer molecules and the hydrophobic regions of phospholipid membranes. DSC thermograms revealed that both the conformational change in the phospholipid headgroups and the disordering in the hydrophobic regions of phospholipid membranes were induced by four guanidine hydrochloride polymers. This was a result of strong interactions of the polymer not only with the polar headgroups of the phospholipid layers, as indicated by changes in the pretransition, but also with the hydrophobic core of the phospholipid membranes, as indicated by cooperativity changes in the main transition. Polymer $C_4$ and $C_{8(benzene)}$ significantly decreased the temperature and enthalpy of pretransition, as well as the temperature of the main transition. Polymer $C_6$ and $C_8$ caused the pretransition disappearance and the increased half-width of the main transition peak. Even Polymer $C_8$ caused a two-component main phase transition. So Polymer $C_4$, $C_{8(benzene)}$, $C_6$, and $C_8$ induced an increasing change extent of DSC thermograms, which correlated to the magnitude of their biocidal ability. It was noteworthy that Polymer $C_8$ induced the largest decrease in the cooperativity of the main phase transition by significantly broadening the transition and decreasing its transition temperature, indicating strongest interactions with the lipid vesicles. The above information corresponded to the highest biocidal activity of Polymer $C_8$. The widest main transition peak and another component at the right wing of the main transition were a consequence of the non-homogeneous distribution of Polymer $C_8$ within the phospholipid membrane. As a result, regions of several coexisting phases, one lipid-rich phase and other phases rich in polymer, could be formed. Just the gradual phase segregation between polymer-poor and polymer-rich domains eventually led to the membrane disruptions. Actually, a mechanism about the formation of membrane domains and the lipid phase segregation was suggested for the antimicrobial mechanism of polycationic antimicrobial agents [21,40]. By using DSC, Cong *et al.* also suggested that the perturbation of anionic phospholipid membrane induced by pirarubicin (an anthracycline antibiotic) might be due to the strong membrane interactions between the pirarubicin and phospholipids [41].

In ITC experiments, the entropically favorable binding of Polymer $C_4$, $C_6$, and C8 to the anionic POPE/POPG membrane could be attributed to the entropy gain of released counterions and liberated solvent molecules, when

two hydrophobic regions come in close contact, thus releasing solvents and small ions. The interpretation was consistent with the report by Gabriel *et al.* [36].

It was reported that highly efficient cationic antibacterial polymers could be obtained by tuning the overall hydrophobicity of the repeat unit of the polymer molecule [42]. We inferred that for Polymer $C_4$, $C_6$, and $C_8$, the gradually increased overall hydrophobicity with the growing aldyl chain length led to their increasing ability to partition into the hydrophobic region of the phospholipid membrane and the increasing binding affinity (evaluated by the binding constant and the energy change) to the membrane, which eventually resulted in these polymers' gradually increased membrane-disrupting ability and biocidal activity. The rigid benzene ring of Polymer $C_{8(benzene)}$ limited its partition into the lipid membrane and led to its weaker membrane-disrupting ability compared with the flexible alkyl chain of Polymer $C_8$.

Extrusion through a 400 nm pore filter was bound to yield oligolamellar vesicles as well, not just unilamellar ones. But the effect on the comparison study could be negligible because the preparation methods of used phospholipid vesicles for different polymer were the same.

In summary, the combined studies by dye-leakage assay, ITC and DSC suggested that the membrane disruption actions of the biocidal guanidine hydrochloride polymers [Polymer $C_4$, $C_6$, $C_8$, and $C_{8(benzene)}$] were resulted from the polymer's strong binding to the phospholipid membrane and the followed perturbations of the polar headgroups and the hydrophobic core of the phospholipid membrane. The alkyl chain structure of polymer $C_4$, $C_6$, $C_8$, and $C_{8(benzene)}$ significantly affects the binding constant and energy change value of thermodynamics of the strong polymer–membrane interactions, the perturbation extent of the polar headgroups and the hydrophobic core of the phospholipid membrane, which lead to their different biocidal activity.

## Supplementary Data

Supplementary data are available at *ABBS* online.

## Acknowledgements

The authors gratefully acknowledge Dr Xiaofei Jiang (Huashan Hospital, Shanghai Medical College, Fudan University) for supplying the clinical strains.

## Funding

This work was supported by grants from the National Natural Science Foundation of China (30821005 and 50573020) and the Shanghai Leading Academic Discipline Project (B203 and B505).

## References

1 Kumarasamy KK, Toleman MA, Walsh TR, Bagaria J, Butt F, Balakrishnan R and Chaudhary U, *et al*. Emergence of a new antibiotic resistance mechanism in India, Pakistan, and the UK: a molecular, biological, and epidemiological study. Lancet Infect Dis 2010, 10: 597–602.
2 Moellering RC. Discovering new antimicrobials agents. Int J Antimicrob Ag 2011, 37: 2–9.
3 Findlay B, Zhanel GG and Schweizer F. Cationic amphiphiles, a new generation of antimicrobials inspired by the natural antimicrobial peptide scaffold. Antimicrob Agents Chemother 2010, 54: 4049–4058.
4 Tew GN, Scott RW, Klein ML and DeGrado WF. De novo design of antimicrobial polymers, foldamers, and small molecules: from discovery to practical applications. Acc Chem Res 2010, 43: 30–39.
5 Lewis K and Klibanov AM. Surpassing nature: rational design of sterile-surface materials. Trends Biotechnol 2005, 23: 343–348.
6 Kenawy ER, Worley SD and Broughton R. The chemistry and applications of antimicrobial polymers: A state-of-the-art review. Biomacromolecules 2007, 8: 1359–1384.
7 Bera S, Zhanel GG and Schweizer F. Antibacterial activity of guanidinylated neomycin B- and kanamycin A-derived amphiphilic lipid conjugates. J Antimicrob Chemother 2010, 65: 1224–1227.
8 Buxbaum A, Kratzer C, Graninger W and Georgopoulos A. Antimicrobial and toxicological profile of the new biocide Akacid plus®. J Antimicrob Chemother 2006, 58: 193–197.
9 Oule MK, Azinwi R, Bernier AM, Kablan T, Maupertuis AM, Mauler S and Nevry RK, *et al*. Polyhexamethylene guanidine hydrochloride-based disinfectant: a novel tool to fight meticillin-resistant *Staphylococcus aureus* and nosocomial infections. J Med Microbiol 2008, 57: 1523–1528.
10 Gilbert P and Moore LE. Cationic antiseptics: diversity of action under a common epithet. J Appl Microbio 2005, 99: 703–715.
11 Zhang YM, Jiang JM and Chen YM. Synthesis and antimicrobial activity of polymeric guanidine and biguandine salts. Polymer 1999, 40: 6189–6198.
12 O'Malley LP, Hassan KZ, Brittan H, Johnson N and Collins AN. Characterization of the biocide polyhexamethylene biguanide by matrix-assisted laser desorption ionization time-of-flight mass spectrometry. J Appl Polym Sci 2006, 102: 4928–4936.
13 Albert M, Feiertag P, Hayn G, Saf R and Honig H. Structure-activity relationships of oligoguanidinessInfluence of counterion, diamine, and average molecular weight on biocidal activities. Biomacromolecules 2003, 4: 1811–1817.
14 Sun SL, An QZ, Li X, Qian LY, He BH and Xiao HN. Synergistic effects of chitosan-guanidine complexes on enhancing antimicrobial activity and wet-strength of paper. Bioresource Technol 2010, 101: 5693–5700.
15 Guan Y, Qian LY, Xiao HN and Zheng AN. Preparation of novel antimicrobial-modified starch and its adsorption on cellulose fibers: Part I. Optimization of synthetic conditions and antimicrobial activities. Cellulose 2008, 15: 609–618.
16 Zhou ZX, Wei DF, Guan Y, Zheng AN and Zhong JJ. Damage of *Escherichia coli* membrane by bactericidal agent polyhexamethylene guanidine hydrochloride: micrographic evidences. J Appl Microbiol 2010, 108: 898–907.
17 Saczewski F and Balewski L. Biological activities of guanidine compounds. Expert Opin Ther Pat 2009, 19: 1417–1448.
18 Thakkar N, Pirrone V, Passic S, Zhu W, Kholodovych V, Welsh W and Rando RF, *et al*. Specific interactions between the viral coreceptor CXCR4 and the Biguanide-based compound NB325 mediate inhibition of

human immunodeficiency virus Type 1 infection. Antimicrob Agents Chemother 2009, 53: 631–638.
19 Pinto F, Maillard JY, Denyer SP and McGeechan P. Polyhexamethylene biguanide exposure leads to viral aggregation. J Appl Microbiol 2010, 108: 1880–1888.
20 Berlinck RGS, Burtoloso ACB and Kossuga MH. The chemistry and biology of organic guanidine derivatives. Nat Prod Rep 2008, 25: 919–954.
21 Epand RM and Epand RF. Lipid domains in bacterial membranes and the action of antimicrobial agents. Biochim Biophys Acta Biomembr 2009, 1788: 289–294.
22 Som A and Tew GN. Influence of lipid composition on membrane activity of antimicrobial phenylene ethynylene oligomers. J Phys Chem B 2008, 112: 3495–3502.
23 Reuter M, Schwieger C, Meister A, Karlsson G and Blume A. Poly-L-lysines and poly-L-arginines induce leakage of negatively charged phospholipid vesicles and translocate through the lipid bilayer upon electrostatic binding to the membrane. Biophys Chem 2009, 144: 27–37.
24 Wang QD, Cui DF and Lin QS. Interaction of the apolipoprotein A-I model peptides with liposomes. Acta Biochim Biophys Sin 1997, 29: 8–16.
25 Andrushchenko VV, Aarabi MH, Nguyen LT, Prenner EJ and Vogel HJ. Thermodynamics of the interactions of tryptophan-rich cathelicidin antimicrobial peptides with model and natural membranes. Biochim Biophys Acta Biomembr 2008, 1778: 1004–1014.
26 Al-Kaddah S, Reder-Christ K, Klocek G, Wiedemann I, Brunschweiger M and Bendas G. Analysis of membrane interactions of antibiotic peptides using ITC and biosensor measurements. Biophys Chem 2010, 152: 145–152.
27 Andrushchenko VV, Vogel HJ and Prenner EJ. Interactions of tryptophan-rich cathelicidin antimicrobial peptides with model membranes studied by differential scanning calorimetry. Biochim Biophys Acta Biomembr 2007, 1768: 2447–2458.
28 Prossnigg F, Hickel A, Pabst G and Lohner K. Packing behaviour of two predominant anionic phospholipids of bacterial cytoplasmic membranes. Biophys Chem 2010, 150: 129–135.
29 Zorko M and Jerala R. Alexidine and chlorhexidine bind to lipopolysaccharide and lipoteichoic acid and prevent cell activation by antibiotics. J Antimicrob Chemother 2008, 62: 730–737.
30 Wayne PA. Methods for Dilution Antimicrobial Susceptibility Tests for Bacteria that Grow Aerobically; Approved Standard. 8th edn. Document M07-A8. Wayne, Pennsylvania, USA: Clinical and Laboratory Standards Institute, 2009.
31 Torchilin VP and Weissig V. Liposomes: A Practical Approach. Oxford: Oxford University Press, 2003.
32 Liang Y, Du F, Sanglier S, Zhou BR, Xia Y, Van Dorsselaer A and Maechling C, *et al*. Unfolding of rabbit muscle creatine kinase induced by acid - A study using electrospray ionization mass spectrometry, isothermal titration calorimetry, and fluorescence spectroscopy. J Biol Chem 2003, 278: 30098–30105.
33 Abbassi F, Galanth C, Amiche M, Saito K, Piesse C, Zargarian L and Hani K, *et al*. Solution structure and model membrane interactions of temporins-SH, antimicrobial peptides from amphibian skin. A NMR spectroscopy and differential scanning calorimetry study. Biochemistry 2008, 47: 10513–10525.
34 Henzler-Wildman KA, Martinez GV, Brown MF and Ramamoorthy A. Perturbation of the hydrophobic core of lipid bilayers by the human antimicrobial peptide LL-37. Biochemistry 2004, 43: 8459–8469.
35 Bastos M, Bai G, Gomes P, Andreu D, Goormaghtigh E and Prieo M. Energetics and partition of two cecropin-melittin hybrid peptides to model membranes of different composition. Biophys J 2008, 94: 2128–2141.
36 Gabriel GJ, Pool JG, Som A, Dabkowski JM, Coughlin EB, Muthukurnar M and Tew GN. Interactions between antimicrobial polynorbornenes and phospholipid vesicles monitored by light scattering and microcalorimetry. Langmuir 2008, 24: 12489–12495.
37 Gottler LM, Bea RD, Shelburne CE, Ramamoorthy A, Marsh E and Neil G. Using fluorous amino acids to probe the effects of changing hydrophobicity on the physical and biological properties of the β-Hairpin antimicrobial peptide protegrin-1. Biochemistry 2008, 47: 9243–9250.
38 Thennarasu S, Lee DK, Tan A, Kari UP and Ramamoorthy A. Antimicrobial activity and membrane selective interactions of a synthetic lipopeptide MSI-843. Biochim Biophys Acta Biomembr 2005, 1711: 49–58.
39 Seelig J. Thermodynamics of lipid-peptide interactions. Biochim Biophys Acta Biomembr 2004, 1666: 40–50.
40 Epand RM, Rotem S, Mor A, Berno B and Epand RF. Bacterial membranes as predictors of antimicrobial potency. J Am Chem Soc 2008, 130: 14346–14352.
41 Cong WJ, Liu QF, Liang QL, Wang YM and Luo GA. Investigation on the interactions between pirarubicin and phospholipids. Biophys Chem 2009, 143: 154–160.
42 Ilker MF, Nüsslein K, Tew GN and Coughlin EB. Tuning the hemolytic and antibacterial activities of amphiphilic polynorbornene derivatives. J Am Chem Soc 2004, 126: 15870–15875.